

# Field and polarity dependence of time-to-resistance increase in Fe–O films studied by constant voltage stress method

Koji Eriguchi,<sup>1,a)</sup> Zhiqiang Wei,<sup>2</sup> Takeshi Takagi,<sup>2</sup> Hiroaki Ohta,<sup>1</sup> and Kouichi Ono<sup>1</sup>

<sup>1</sup>Graduate School of Engineering, Kyoto University, Yoshida-Honmachi, Sakyo-ku, Kyoto 606-8501, Japan

<sup>2</sup>Advanced Device Development Center, Matsushita Electric Ind. Co., Ltd., 3-1-1 Yagumo-Nakamachi, Moriguchi, Osaka 570-8501, Japan

(Received 7 August 2008; accepted 12 December 2008; published online 8 January 2009)

Constant voltage stress (CVS) was applied to Fe–O films prepared by a sputtering process to investigate a stress-induced resistance increase leading to a fundamental mechanism for switching behaviors. Under the CVS, an abrupt resistance increase was found for both stress polarities. A conduction mechanism after the resistance increase exhibited non-Ohmic transport. The time-to-resistance increase ( $t_r$ ) under the CVS was revealed to strongly depend on stress voltage as well as the polarity. From a polarity-dependent resistance increase determined by a time-zero measurement, the voltage and polarity-dependent  $t_r$  were discussed on the basis of field- and structure-enhanced thermochemical reaction mechanisms. © 2009 American Institute of Physics. [DOI: 10.1063/1.3064127]

With an increasing demand in advanced microelectronic memory devices, resistive random access memories (ReRAMs) have become one of the most promising candidates replacing present-day nonvolatile memories. Various binary-oxide materials such as TiO<sub>2</sub>,<sup>1</sup> NiO,<sup>2,3</sup> CoO,<sup>4</sup> ZrO,<sup>5</sup> and FeO<sup>6</sup> were extensively investigated for ReRAM applications. Recently, the resistive switching behaviors in the above materials have been reported and the switching mechanisms have been studied from various aspects.<sup>2,3,6–8</sup> In terms of reliability assessments for memory devices, data retention and endurance characteristics are primal concerns and the related issues have been widely discussed. However, compared with a time-dependent dielectric breakdown of SiO<sub>2</sub> (gate dielectric material)<sup>9,10</sup> in metal-oxide-semiconductor field effect transistors (MOSFETs), which has been extensively studied, there have been few reports on a time-dependent structural change by a constant electrical stress inducing a resistance change. In order to predict correctly a reliable lifetime for designed operation such as data retention and endurance characteristics, the fundamental understanding of time-dependent resistance change behavior by using a constant stress measurement widely conducted in studies of SiO<sub>2</sub> breakdown<sup>9–11</sup> is significant and the underlying mechanism should be clarified. In this paper, a time-dependent resistance change in Fe–O-based films (denoted here as Fe–O) is comprehensively investigated by using a constant voltage stress (CVS) with different polarities.<sup>12,13</sup>

An Fe–O film with a thickness of 100 nm was deposited by rf magnetron sputtering process at 400 °C under a pressure of 2.0 Pa using an Fe<sub>3</sub>O<sub>4</sub> target. No subsequent annealing was performed for samples tested in this study. As-deposited initial film was identified as stoichiometric Fe<sub>3</sub>O<sub>4</sub>-containing film from Fourier transform infrared spectrum. The Fe–O film was sandwiched between the top and bottom Pt electrodes with a thickness of 100 nm. The area of Fe–O film was 0.5 × 0.5 μm<sup>2</sup>. Details of the fabrication process and test structure were reported

elsewhere.<sup>6</sup> Another Fe–O-based film with multilayer structure (Fe<sub>3</sub>O<sub>4</sub>/Fe<sub>2</sub>O<sub>3</sub>/Fe<sub>3</sub>O<sub>4</sub>=47.5/5.0/47.5 nm) prepared by the same magnetron sputtering process chamber at 400 °C was also evaluated for comparison. All the electrical measurements were performed at room temperature. To investigate time-dependent resistance change, we applied a constant voltage ( $V_{st}$ ) stress with different polarities, i.e., a positive  $V_{st}$  corresponds to the electron injection from bottom electrode and a negative  $V_{st}$  to that from top electrode. With regard to the Fe–O films used in this study, the switching behavior was achieved by an optimized electroforming process (usually a pulsed stress with the duration of ~1 μs).<sup>6</sup> For the purpose of investigating the fundamental characteristics, samples without the electroforming process were used. As will be discussed later in this article, the resistance increase was found for the samples without the electroforming processes by applying the voltage different from that for an electroforming. Note that the input energy to the film in CVS tests is higher than that in the electroforming. With an injected current under CVS [ $I_{CVS}(t)$ ] being monitored, the time-to-resistance increase ( $t_r$ ) was judged as a sudden change in resistance ( $R$ ):  $\Delta I_{CVS}/I_{CVS} > 50\%$ . We found that the higher  $V_{st}$  induced the larger resistance increase. Note that the judgment in the above is used for time-dependent dielectric breakdown assessment of an SiO<sub>2</sub> (Refs. 11–13) and other dielectric layers to predict a reliability lifetime in MOSFETs.

Figure 1 shows current-voltage characteristics for the initial and higher-resistance structures. The vertical axis on the left is an initial current ( $I_0$ ) and that on the right, the current of higher-resistance device ( $I_{rc}$ ), as a function of applied voltage ( $V_b$ ). In order to induce the resistance change, an applied voltage ( $|V_b|$ ) was swept from 0 to 5.0 V. The abrupt decrease in the current was observed at ~4.0 V, as shown in the inset. An Ohmic behavior is seen in fresh devices, while  $I_{rc}$  does not exhibit a linear relationship with  $V_b$ , i.e., non-Ohmic conduction, indicating an existence of insulating layer between the electrodes. It has been reported that a switching behavior by Fe–O film for ReRAM application is attributed to a crystalline structure change based on the redox reaction  $2Fe_3O_4 + O_2 \rightarrow 3\gamma-Fe_2O_3 + 2e^-$ . Thus, the observed

<sup>a)</sup>Tel.: +81-75-753-5983. Electronic address: eriguchi@kuaero.kyoto-u.ac.jp.

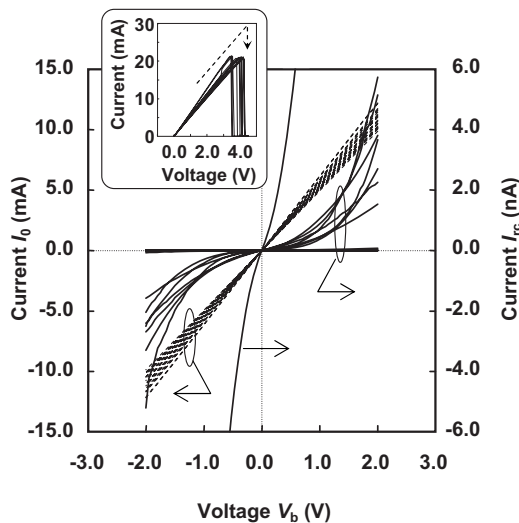


FIG. 1. Current vs voltage characteristics for Fe–O films. The vertical axis on the left is an initial current ( $I_0$ ; dotted lines) and that on the right is the current for various resistance-changed devices ( $I_{rc}$ ; solid lines). Example for the resistance change process is shown in the inset.

$I_{rc}$ - $V_b$  characteristic in Fig. 1 is due to a  $\gamma$ -Fe<sub>2</sub>O<sub>3</sub> layer (an insulator) formation on the anode interface (the bottom electrode interface for  $V_b < 0$ ), which will be discussed later.

Owing to the  $\gamma$ -Fe<sub>2</sub>O<sub>3</sub> layer formation<sup>6</sup> (higher resistance layer compared with Fe<sub>3</sub>O<sub>4</sub> layer) by CVS, the resistance of the structures with the  $\gamma$ -Fe<sub>2</sub>O<sub>3</sub> layer near the anode interface is expected to increase with stress time (with an increase in the thickness). An example of time evolution of  $I_{CVS}(t)$ , i.e., the resistance [ $R(t)$ ] is shown in Fig. 2 for negative and positive stress polarities. The abrupt increase in  $R(t)$  is seen. (Note that the samples show no switching behavior since the CVS with a single polarity was kept to be applied in this study.) For example, we estimate the increase in  $R(t)$  from  $\sim 160 \Omega$  (initial stage) to  $\sim 5500 \Omega$  (destructive stage) at  $V_{st} = -2.2$  V. The increase in  $R(t)$  regardless of the polarity is attributed to fundamental degrading feature of Fe–O films associated with the  $\gamma$ -Fe<sub>2</sub>O<sub>3</sub> layer formation near the anode interface. The increase in resistance by CVS is consistent to that by electroforming while the value of the incre-

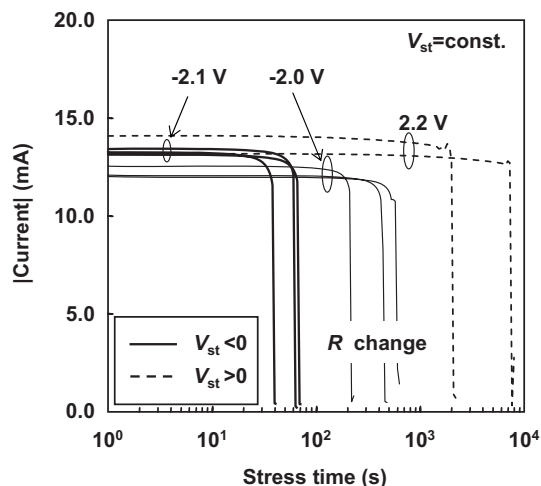


FIG. 2. Examples of time evolution of injected current under a constant voltage stress [ $I_{CVS}(t)$ ] for various stress conditions with different polarities. Time-to-resistance change ( $t_r$ ) is judged as the change in  $I_{CVS}(t)$ , respectively.

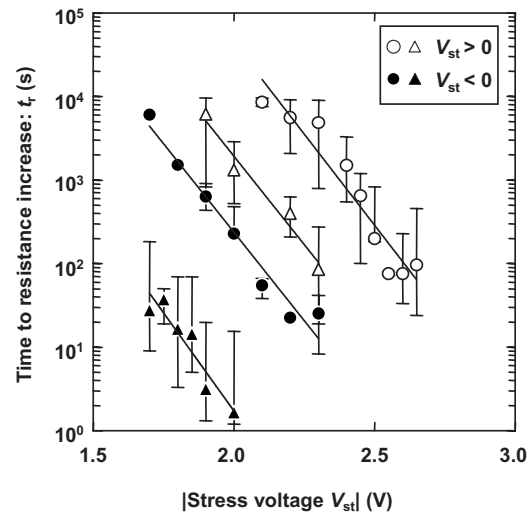


FIG. 3. Time-to-resistance increase ( $t_r$ ) as a function of stress voltage for various stress conditions with different polarities (positive stress: open circle, negative stress: closed circle.) The  $t_r$  for Fe–O multilayer structure is also shown for comparison. (positive stress: open triangle, negative stress: closed triangle.)

ment is different. This may be due to the difference in input energy between  $V_{st}$  and a pulsed stress voltage for the electroforming, resulting in the difference in film structure changes by Joule-heating effect.<sup>2</sup> The higher input energy by CVS might lead to forming the different high-resistive film structures, in other words, the different states in free-energy coordinates<sup>10</sup> from microscopic viewpoints. Details are hoped to be clarified in the future. However, we consider that the resistance increase in Fig. 2 implies a fundamental mechanism of structural changes in the films near the anode interface.<sup>6</sup> From the above new findings, one can discuss a basic resistance increase mechanism as follows. Here we define time-to-resistance increase ( $t_r$ ) in accordance with the abrupt increase for each stress configuration as in Fig. 2.  $t_r$  is determined from the median among more than six different devices. Toward  $t_r$ , one can also see the decrease in  $I_{CVS}(t)$ , i.e., the increase in  $R(t)$ . Since the increase in  $R(t)$  is due to the  $\gamma$ -Fe<sub>2</sub>O<sub>3</sub> layer formation on the anode electrode by the redox reaction of Fe<sub>3</sub>O<sub>4</sub>, this steep increase is attributed to an increase in the  $\gamma$ -Fe<sub>2</sub>O<sub>3</sub>-layer thickness (an increase in the tunneling distance for electrons), resulting in an exponential increase in the resistance.

Figure 3 summarizes the dependences of  $t_r$  on  $V_{st}$ , respectively, for negative and positive stress polarities. Two important features are seen. (1)  $t_r$  strongly depends on  $V_{st}$ . By extrapolating the obtained relationship, one can foresee a limited lifetime in the presence of the electrical stress at a voltage derived from device operation. (2) Negative stress polarity decreases  $t_r$ , i.e., accelerates the time-to-resistance increase. The same trends are observable for different film structures, as also shown in Fig. 3. With regard to a field-enhanced acceleration for resistance increase, we can estimate a voltage-acceleration factor  $\beta$  from the fitted curves shown in Fig. 3. By a least-squares fit with the assumption of  $t_r \propto \exp(-\beta V_{st})$ ,  $\beta$  is determined as 9.2 and 9.8 V<sup>-1</sup> in the case of single Fe<sub>3</sub>O<sub>4</sub> film for positive and negative  $V_{st}$ , respectively, and as 9.8 and 10.8 V<sup>-1</sup> in the case of multilayer structure (Fe<sub>3</sub>O<sub>4</sub>/Fe<sub>2</sub>O<sub>3</sub>/Fe<sub>3</sub>O<sub>4</sub>) for positive and negative  $V_{st}$ , respectively. The obtained values are close to each other,

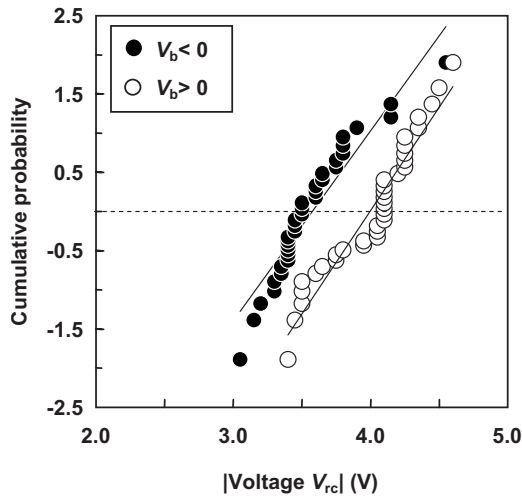


FIG. 4. Cumulative probabilities of a critical voltage for the resistance change ( $V_{rc}$ ) with different stress polarities.

indicating that the observed field-enhanced resistance increase is governed by the same fundamental mechanism. By applying a thermochemical model, the time-to-resistance increase ( $t_r$ ) associated with  $O_2$  diffusion and reaction<sup>6</sup> is determined by the reaction rate constant  $k$ :  $k \propto \exp(-H/k_B T)$ , where  $k_B$  is Boltzmann's constant,  $T$  is the temperature, and  $H$  is the enthalpy for the reaction usually referred to as activation energy, depending on test structures, materials, and electric field. Thus  $t_r$  is described by  $t_r \propto k^{-1} \propto \exp(H/k_B T)$ . By assuming that  $H_0$  is an amount of energy required for the transition from high resistance to low resistance state in the absence of field, then in the presence of field in Fe-O film ( $E_{st}$ ),  $H$  is described by  $H = H_0 - aE_{st} - b = H_0 - aV_{st}/d - b$ , where  $b$  is a structure-dependent parameter,  $d$  is a thickness of the film, and  $a$  corresponds to a field-enhancement factor<sup>10</sup> related to the Fe-O bond, giving  $a \sim 2.5 \times 10^2 \text{ e \AA}$  with  $T = 300 \text{ K}$  in this case. The parameters  $a$  and  $b$  control the reaction rate. Based on the proposed model, a stress voltage dependence is determined by  $t_r \propto \exp(-\beta V_{st}) \propto \exp(-aV_{st}/dk_B T)$ .

Now we focus on the polarity dependence, i.e., the decrease in  $t_r$  itself for negative stress voltage for Fe-O film in Fig. 3. The ratio of  $t_r$  for the negative to that for the positive polarity ( $R_{tr}$ ) is calculated from the least-squares fitted lines as  $\sim 0.030$ . This value corresponds to the difference in the aforementioned parameter  $b$  between the negative and positive stress ( $\Delta b$ ): From  $R_{tr}$ ,  $H$  under the negative voltage configuration is considered to be lower by  $\Delta H = \Delta b = k_B T \ln(R_{tr}) \sim 0.09 \text{ eV}$  than that under the positive. By taking into account the fact that the time-to-breakdown of thin  $SiO_2$  film in MOSFETs is controlled by a mechanical strain developing at the Si substrate interface,<sup>14</sup> we assume that the anode interface property at the top (in the case of  $V_{st} > 0$ ) or bottom (in that of  $V_{st} < 0$ ) electrodes determines the parameter  $b$  in  $H$  in this estimation, respectively. This value can be verified by the critical voltage ( $V_{rc}$ ) for the resistance change under negative and positive stress measurements, respectively, as shown in Fig. 4. Figure 4 shows cumulative probability of  $V_{rc}$ , the so-called time-zero measurement.<sup>15</sup>  $V_{rc}$  was

judged by a sudden decrease in  $|V_b|$  during the bias voltage sweep as shown in the inset of Fig. 1. As seen in Fig. 4, the decrease in  $|V_{rc}|$  under the negative stress ( $\Delta V_{rc}$ ) can be determined as 0.42 V from the shift in fitted lines. Since a  $\gamma\text{-Fe}_2\text{O}_3$  layer formation near the anode interface is deduced as a thermochemical reaction process,  $\Delta V_{rc}$  corresponds to a difference in  $H$  by  $\sim 0.10 \text{ eV}$  ( $=k_B T \times \beta \Delta V_{rc}$ ) on the basis of the proposed model. We speculate that this estimated value derives from a difference in the structure-dependent parameter  $b$ , consistent with the value ( $\Delta b \sim 0.09 \text{ eV}$ ) determined from the  $R_{tr}$  or the decrease in  $t_r$  in Fig. 3. The observed polarity dependence of  $t_r$  for both films structures is attributed to the difference of  $b$  ( $\Delta b$ ) associated with the anode interface property and implies that the interface structure is responsible for a resistance switching behavior. Moreover, the observed decreases in polarity-dependent  $t_r$  and  $|V_{rc}|$  are considered to be due to the Fe-O sputtering process-induced damage at the Pt bottom electrode surface. Thus, the time-dependent resistance change (increase) is controlled by the thermochemical process, i.e., the field-enhanced reaction rate as well as interface property.

In summary, by using a continuous constant voltage stress, we have revealed the strong field- and polarity-dependent resistance increase in Fe-O films. Based on the present findings, the correlation between the polarity dependence of  $t_r$  and that of  $V_{rc}$  was clarified. It was confirmed that the process is controlled by a thermochemical reaction mechanism. The present method with simple stress configurations provides a significant implication for a resistance change (switching behavior) in materials for ReRAM application as well as a key consideration for the reliability assessment under various operations.

- <sup>1</sup>M. Fujimoto, H. Koyama, Y. Hosoi, K. Ishihara, and S. Kobayashi, *Jpn. J. Appl. Phys., Part 2* **45**, L310 (2006).
- <sup>2</sup>U. Russo, D. Ielmini, C. Cagil, A. L. Lacaite, S. Spiga, C. Wiemer, M. Perego, and M. Fanciulli, *Tech. Dig. - Int. Electron Devices Meet.* **2007**, 775.
- <sup>3</sup>K. Tsunoda, K. Kinoshita, H. Nishiro, Y. Yamazaki, T. Iizuka, Y. Ito, A. Takahashi, A. Okano, Y. Sato, T. Fukano, M. Aoki, and Y. Sugiyama, *Tech. Dig. - Int. Electron Devices Meet.* **2007**, 767.
- <sup>4</sup>H. Shima, F. Takano, Y. Tamai, H. Akinaga, and I. H. Inoue, *Jpn. J. Appl. Phys., Part 2* **46**, L57 (2007).
- <sup>5</sup>D. Lee, H. Choi, H. Sim, D. Choi, H. Hwang, M.-J. Lee, S.-A. Seo, and I. K. Yoo, *IEEE Electron Device Lett.* **26**, 719 (2005).
- <sup>6</sup>S. Muraoka, K. Osano, Y. Kanzawa, S. Mitani, S. Fujii, K. Katayama, Y. Katoh, Z. Wei, T. Mikawa, K. Arita, Y. Kawashima, R. Azuma, K. Kawai, K. Shimakawa, A. Odagawa, and T. Takagi, *Tech. Dig. - Int. Electron. Devices Meet.* **2007**, 779.
- <sup>7</sup>I. G. Baek, M. S. Lee, S. Seo, M. J. Lee, D. H. Seo, D.-S. Suh, J. C. Park, S. O. Park, H. S. Kim, I. K. Yoo, U.-I. Chung, and J. T. Moon, *Tech. Dig. - Int. Electron. Devices Meet.* **2004**, 587.
- <sup>8</sup>M. J. Rozenberg, I. H. Inoue, and M. J. Sanchez, *Phys. Rev. Lett.* **92**, 178302 (2004).
- <sup>9</sup>J. W. McPherson and D. A. Baglee, *J. Electrochem. Soc.* **132**, 1903 (1985).
- <sup>10</sup>J. W. McPherson and H. C. Mogul, *J. Appl. Phys.* **84**, 1513 (1998).
- <sup>11</sup>K. Eriguchi and Y. Kosaka, *IEEE Trans. Electron Devices* **45**, 160 (1998).
- <sup>12</sup>K. Eriguchi and M. Niwa, *IEEE Electron Device Lett.* **19**, 399 (1998).
- <sup>13</sup>K. Eriguchi and M. Niwa, *Appl. Phys. Lett.* **73**, 1985 (1998).
- <sup>14</sup>K. Eriguchi, Y. Harada, and M. Niwa, *J. Appl. Phys.* **87**, 1990 (2000).
- <sup>15</sup>A. Berman, *IEEE Proceedings of the International Reliability Physics Symposium*, 1981, p. 204.